

Possible origin of the slow-diffusion region around Geminga

Kun Fang^{1*} Xiao-Jun Bi^{1,2†} Peng-Fei Yin^{1‡}

¹ Key Laboratory of Particle Astrophysics, Institute of High Energy Physics, Chinese Academy of Sciences, Beijing 100049, China

² School of Physical Sciences, University of Chinese Academy of Sciences, Beijing 100049, China

15 December 2024

ABSTRACT

Geminga pulsar is surrounded by a multi-TeV γ -ray halo radiated by high energy electrons and positrons accelerated by the central pulsar wind nebula (PWN). The angular profile of the γ -ray emission reported by HAWC indicates an anomalously slow diffusion for cosmic-ray electrons and positrons in the halo region around Geminga. In the paper we study the possible mechanism for the origin of slow diffusion. At first, we consider the self-generated Alfvén waves due to streaming instability of the electrons and positrons released by Geminga. However, even considering a very optimistic scenario for the wave growth, we find this mechanism DOES NOT work to account for the extremely slow diffusion at the present day if taking the proper motion of the pulsar into account. The reason is straightforward as the PWN is too weak to generate enough high energy electrons and positrons to stimulate strong turbulence at the late time. We then propose an assumption that the strong turbulence is generated by the shock wave of the parent supernova remnant of Geminga. Geminga may still be in the downstream region of the shock wave and embedded in a slow-diffusion circumstance. The TeV halos around PSR B0656+14 and Vela X may also be explained under this assumption.

Key words: cosmic rays – ISM: individual objects: Geminga nebula – ISM: supernova remnants – turbulence

1 INTRODUCTION

The well-known γ -ray pulsar Geminga is surrounded by a multi-TeV γ -ray halo, which was first detected by Milagro (Abdo et al. 2007). In late 2017, the High-Altitude Water Cherenkov Observatory (HAWC) collaboration further reported the spatially resolved observation of the γ -ray halo (Abeysekara et al. 2017a). As these very-high-energy (VHE) γ rays are emitted by electrons and positrons¹ mainly through inverse Compton scattering of the cosmic microwave background photons, the surface brightness profile of the γ -ray emission can be a good indicator for the propagation of electrons near the source. However, the derived diffusion coefficient of ~ 60 TeV² electrons is hundreds times slower than

the average value in the Galaxy as inferred from the boron-to-carbon ratio (B/C) measurements (Aguilar et al. 2016). This is an evidence that the diffusion coefficient may be highly inhomogeneous in small scale. Investigating the origin of this slow-diffusion region could be meaningful to understand the particle propagation near cosmic-ray sources.

A plausible explanation is that the relatively large particle density near the source may lead to the resonant growth of Alfvén waves, which in turn scatter the particles and therefore suppress the diffusion velocity (Ptuskin et al. 2008; Malkov et al. 2013; D’Angelo et al. 2016). Based on this mechanism, the diffusion coefficient around Geminga can be significantly reduced in the case of a hard injection spectrum of electrons and a weak ambient magnetic field (this calculation is presented in Appendix A. See also Evoli et al. (2018)). However, the precondition of this interpretation is that Geminga need to be at rest so that the plenty of electrons produced in the early age of Geminga could create a slow-diffusion environment. While due to the proper motion of Geminga, it has already left 70 pc away from its birthplace (Faherty et al. 2007), which means the observed slow-diffusion region must not be formed in the early stage of Geminga. The injection power of Geminga in the present

* fangkun@ihep.ac.cn

† bixj@ihep.ac.cn

‡ yinpf@ihep.ac.cn

¹ Electrons will denote both electrons and positrons hereafter in this paper.

² The average energy of the γ rays observed by HAWC is 20 TeV. Considering the inverse Compton scattering process and the energy spectrum of the parent electrons, 60 TeV electrons contribute most to the γ rays of 20 TeV.

day should be much weaker than that in the early time, and we will show that the diffusion coefficient cannot be remarkably suppressed even in the absence of wave dissipation.

Apart from the self-generated scenario, the slow-diffusion region around Geminga may also be a pre-existing structure. The diffusion coefficient inside a supernova remnant (SNR) should be significantly smaller than that of the interstellar medium (ISM), as this region has been swept by the blast wave and acquired more turbulent energy. So if Geminga is still inside its associated SNR, it could be embedded in a region with small diffusion coefficient, which may explain the observed γ -ray halo. As Geminga may have a 70 pc offset from its birthplace at the present day, there are works considering that Geminga has already left behind its associated SNR. However, we will show below that if the progenitor of Geminga is in a rarefied circumstance, the present scale of the SNR could be large enough to include Geminga in. In the light of this explanation, the problems encountered in the self-confinement scenario could be avoided.

In this work, we first test the self-confinement picture in Section 2 with very optimistic assumptions, including the disregard of the wave dissipation. We consider the impacts brought by the proper motion of Geminga, which is an unavoidable factor. Then in Section 3, we introduce in detail the new interpretation of the inefficient diffusion halo, in which the electrons injected by Geminga are diffusing in the turbulent environment inside its parent SNR. In Section 4, we give some further discussion about this topic, including a brief analysis of some other TeV inefficient diffusion halos, and an alternative scenario of the pre-existing kind of origin for the Geminga halo. Finally, we conclude in Section 5.

2 THE SELF-CONFINED DIFFUSION SCENARIO

A large density gradient of cosmic-ray particles can induce the streaming instability, which may amplify the Alfvén waves in background plasma (Skilling 1971). To derive the diffusion coefficient in the vicinity of a source, we must simultaneously solve the equations of particle transportation and the evolution of the Alfvén waves. A full numerical solution of the coupled equations is presented in Appendix A. Here we only show an optimistic scenario for the turbulence growth where the energy loss of electrons and the Alfvén wave dissipation are ignored. The analysis shows clearly why the self-generated mechanism cannot work to stimulate the turbulence.

We neglect the radiative energy loss of electrons, which leads to a larger gradient of the number density of electrons. Then the propagation equation is expressed as

$$\frac{\partial N}{\partial t} - \nabla \cdot (D \nabla N) = Q, \quad (1)$$

where N is the differential number density of electrons, D is the diffusion coefficient, and Q is the source function.

The energy density of Alfvén waves is denoted with W , which is defined by $\int W(k) dk = \delta B^2 / B_0^2$, where k is the wave number, B_0 is the regular magnetic field strength, and δB is the turbulent magnetic field. Here we ignore the wave dissipation and only consider the growth of the Alfvén waves through streaming instability. The evolution of W can be

then calculated by

$$\frac{\partial W}{\partial t} = \Gamma_{\text{cr}} W = -\frac{4\pi v_A E_{\text{res}}^2}{3B_0^2 k} \nabla N(E_{\text{res}}), \quad (2)$$

where $\Gamma_{\text{cr}} = -4\pi v_A E_{\text{res}}^2 / (3B_0^2 k W) \nabla N(E_{\text{res}})$ is the growth rate according to Skilling (1971), v_A is the Alfvén velocity, and E_{res} is the energy of electrons satisfying $r_g(E_{\text{res}}) = 1/k$, where r_g is the Larmor radius of electrons. The diffusion coefficient is related with W by (Skilling 1971)

$$D(E_{\text{res}}) = \frac{1}{3} r_g c \cdot \frac{1}{k W(k)}. \quad (3)$$

Combining Equation (2) and (3), we get

$$\frac{1}{D^2} \frac{\partial D}{\partial t} = \frac{4\pi e v_A E}{B c} \nabla N. \quad (4)$$

If Geminga is initially in a typical environment of ISM with $\delta B \ll B_0$, the diffusion coefficient along the magnetic field lines should be about $(\delta B / B_0)^{-4}$ times larger than the cross-field diffusion coefficient (Drury 1983). So the propagation of electrons should be initially in a tube of regular magnetic field lines, corresponding to a one-dimensional diffusion. We set x as the coordinate along the regular magnetic field lines, and we get the following expression from Equation (1) and (4):

$$\frac{\partial}{\partial t} \left(N - \frac{B c}{4\pi e v_A E} \frac{\partial \ln D}{\partial x} \right) = \delta(x) \dot{Q}(t), \quad (5)$$

where we assume Geminga is a point-like source, and $\dot{Q}(t)$ is the time profile of electron injection. Then for any $x > 0$, it can be derived from Equation (5) that

$$N - \frac{B c}{4\pi e v_A E} \frac{\partial \ln D}{\partial x} = 0. \quad (6)$$

Integrating Equation (6) from x to ∞ , we finally obtain

$$D(x) = D_{\text{ISM}} \exp \left(-\frac{4\pi e v_A E}{B_0 c} \int_x^\infty N dx' \right), \quad (7)$$

with $D_{\text{ISM}} = D(\infty)$.

Geminga has a proper motion of about 200 km s⁻¹ (Faherty et al. 2007), and the direction of motion is suggested to be nearly transverse to the line of sight (Caraveo et al. 2003). These indicate that Geminga has left its birthplace for about 70 pc now. Meanwhile, the motion of Geminga is almost perpendicular to the Galactic disk (Gehrels & Chen 1993). This means that Geminga has been cutting the magnetic field lines of ISM, as the magnetic field in the Galactic disk is dominated by the horizontal component (Han & Qiao 1994). Thus, the electrons injected in the early age of Geminga should have escaped along the magnetic field lines which is almost perpendicular to the path of Geminga motion and can not help to generate the present slow-diffusion region. In other words, the slow-diffusion region around Geminga observed today must be formed in the recent age if the region is self-excited by Geminga.

We assume the electrons injected during the last third of the age of Geminga (228 kyr~342 kyr) contribute to the generation of the current slow-diffusion region; this should also be an optimistic assumption considering the very fast energy loss of high energy electrons. The injection time function is set to have the same profile with the spin-down luminosity of pulsar, which leads to $\dot{Q}(t, E) = \dot{Q}_0 (1 + t/\tau_0)^{-2} E^{-\gamma}$, where

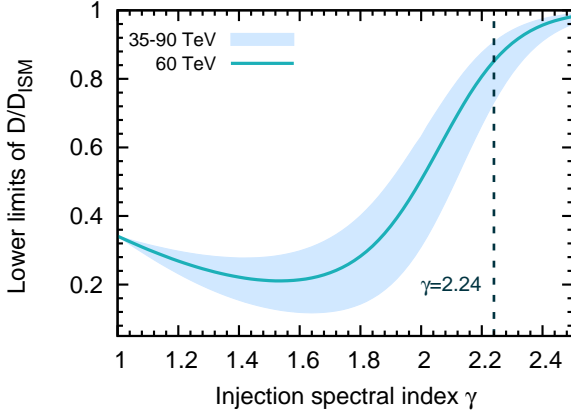


Figure 1. The lower limits of the diffusion coefficient around Geminga under the self-confinement scenario. The solid line is the case of 60 TeV, which is the mean energy of the parent electrons of the γ rays observed by HAWC. The band shows the lower limits of diffusion coefficient varying from 35 to 90 TeV, corresponding to the energy range of HAWC observation. The dotted line marks the injection spectral index provided by HAWC.

$\tau_0 = 10$ kyr (Hooper et al. 2017). We assume all the spin-down energy of Geminga pulsar is converted to the injected electrons with energy from 1 GeV to 500 TeV, to determine the normalization Q_0 . As we have neglected the energy loss of electrons, the following relation can be obtained according to particle conservation:

$$2S \int_x^\infty N(x', E) dx' < \int_{t_1}^{t_2} \dot{Q}(t', E) dt', \quad (8)$$

where $t_1 = 228$ kyr, $t_2 = 342$ kyr, and S is the cross-section of the magnetic flux tube which is assumed to have a scale of 1 pc. Combining Equation (7) and (8), we can then calculate the lower limit of the diffusion coefficient.

The Alfvén velocity is decided by B_0 and the ion density ρ_i as $v_A = B_0 / \sqrt{4\pi\rho_i}$. Then Equation (7) indicates that $D(x)$ is independent of B_0 in our calculation. Considering the morphology of the bow-shock structure observed in X-ray (Caraveo et al. 2003) and the latest distance measure of Geminga (Faherty et al. 2007), the ISM density around Geminga ρ_{ISM} is derived to be $0.02 \text{ atoms cm}^{-3}$. Since the ionization around Geminga is very high (Caraveo et al. 2003), we have $\rho_i \approx \rho_{\text{ISM}}$. The injection spectral index γ cannot be well constrained, as HAWC provides only the energy-integrated result at present.

In Figure 1, we present the lower limits of diffusion coefficient for varying γ . When $\gamma \approx 2.24$ as provided by HAWC, we have $D(60 \text{ TeV}) > 0.85 D_{\text{ISM}}(60 \text{ TeV})$. For 60 TeV particles, the minimum of the lower limit appears at $\gamma = 1.54$, where $D(60 \text{ TeV}) > 0.21 D_{\text{ISM}}(60 \text{ TeV})$. However, this is still too far from the level of suppression required by HAWC observation, which is only about 10^{-3} of the normal diffusion value in ISM as determined by fitting the latest B/C value in Yuan et al. (2017). Therefore it is clearly shown that the self-confinement mechanism cannot serve as the main reason for the suppression of $D(\sim 60 \text{ TeV})$ around Geminga.

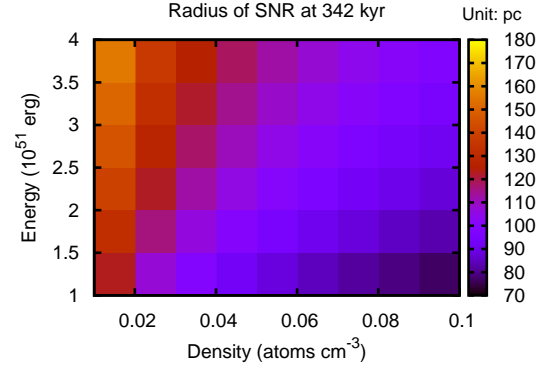


Figure 2. The radius of SNR at an age of 342 kyr, with varying explosion energy and ambient mass density. The calculator provided by Leahy & Williams (2017) is applied to get this figure.

3 ELECTRON AND POSITRON DIFFUSION INSIDE THE SNR

In the SNR shock frame, the upstream plasma loses part of kinetic energy when streaming through the shock front, and this part of energy is transferred into turbulence and thermal energy behind the shock (Bell 1978). Thus, the downstream region should be highly turbulent, although the turbulence may be gradually dissipated after the passage of the shock. So if Geminga is still inside its associated SNR, the slow-diffusion region around it may be explained.

We first give an estimate of the possible scale of the Geminga parent SNR. We adopt the calculator provided by Leahy & Williams (2017). This implement is created for modeling the evolution of SNR, and consistently combines different models for different stages of SNR evolution. The dynamic evolution of SNR is decided by the parameters such as the initial energy of the ejecta E_0 and the density of the ISM n_{ISM} . Figure 2 shows the radius of an SNR at the age of Geminga (342 kyr), with different E_0 and n_{ISM} . The ejecta mass is fixed at $1.4M_\odot$. We find that if the ambient density is relatively low and the initial energy is higher than the typical value of $1 \times 10^{51} \text{ erg}$, the scale of SNR can be as large as ~ 100 pc. The corresponding shock temperature is about 10^5 K , and the temperature inside the SNR should be higher. This is consistent with the high ionization degree around the pulsar wind nebula (PWN) of Geminga, as indicated by the measurement of H α luminosity (Caraveo et al. 2003). As mentioned above, Geminga has left its birthplace for about 70 pc now. Considering the scale of the observed Geminga halo (~ 20 pc), we may envisage a scenario in which Geminga has been chasing the shock wave of its SNR, as presented in the left of Figure 3.

We assume the turbulence is generated just behind the shock with an initial wave spectrum $W_{\text{ini}}(k)$, and the wave transport in the downstream region can be described by

$$\begin{cases} \frac{\partial W}{\partial t} + u_2(t) \frac{\partial W}{\partial x} = -\Gamma_{\text{dis}} W, \\ W(t, 0) = W_{\text{ini}}(t). \end{cases} \quad (9)$$

where the shock rest frame is adopted ($x > 0$ for the downstream region), and u_2 is the downstream fluid ve-

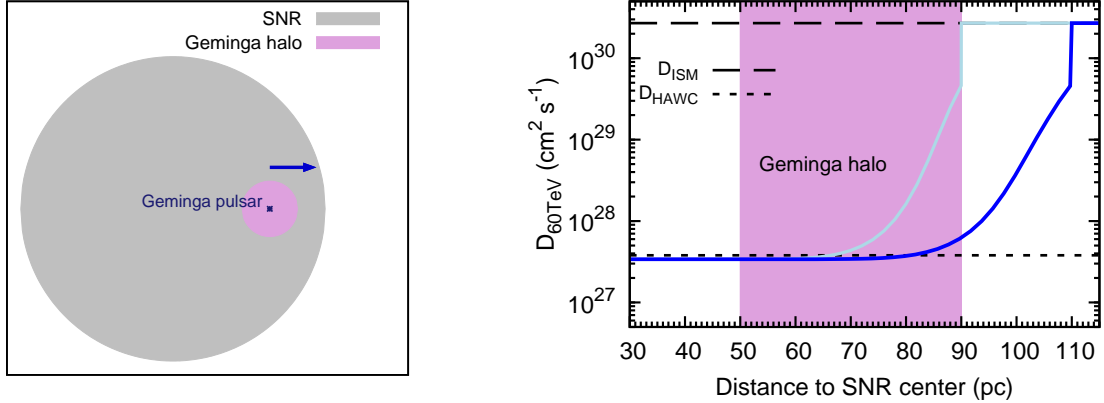


Figure 3. Left: the sketch of the scenario introduced in Section 3. The arrow denotes the direction of the proper motion of Geminga. Right: the spatial distribution of $D(60 \text{ TeV})$ at the present day under the assumption that Geminga is still in its associated SNR. The blue line describes the case in which the current scale of the SNR is 110 pc; the case with a current radius of 90 pc is also shown in light blue for comparison.

locity. The calculator of Leahy & Williams (2017) provides the time-dependent shock speed $v_s(t)$, $u_2(t)$ can be then estimated with $u_2 \approx v_s/4$. We assume the wave dissipation is dominated by the non-linear Landau damping (Cesarsky & Kulsrud 1981), since the ion-neutral damping is not significant for a high ionization environment (Kulsrud & Cesarsky 1971). The simplified dissipation rate of the Kolmogorov type non-linear damping is given by (Ptuskin & Zirakashvili 2003):

$$\Gamma_{\text{dis}} = (2C_K)^{-3/2} v_A k^{3/2} W^{1/2}, \quad (10)$$

where $C_K \approx 3.6$. The initial wave spectrum just behind the shock is assumed to be the Kolmogorov type as $W_{\text{ini}}(k, t) = W_0(t)k^{-5/3}$, where W_0 is the time-dependent normalization. As the turbulent energy downstream is extracted from the kinetic energy of the upstream plasma, we may have $\delta B^2 \sim v_s^2$ just behind the shock. Therefore it is reasonable to assume that $W_0(t) \sim [v_s(t)]^2$. We search for the best $W_0(t)$ so that the average $D(60 \text{ TeV})$ in the Geminga halo (50–90 pc from the SNR center) is consistent with the result of HAWC. Meanwhile, López-Coto & Giacinti (2018) pointed out that the HAWC observation of Geminga halo favors an rms magnetic field of $3 \mu\text{G}$, and a coherence length of the magnetic field of $\sim 1 \text{ pc}$, which corresponds to an outer scale of $\sim 5 \text{ pc}$ for Kolmogorov turbulence. These indicate $B_0 = 0.6 \mu\text{G}$, and $\delta B/B_0 > 1$ in the present Geminga halo.

The wave damping rate given by Equation (9) is proportional to v_A , which is small for our case as $v_A = 9.2 \times 10^5 \text{ cm s}^{-1}$. This means the downstream wave dissipation is relatively slow. We will show below that the damping of the waves inside the SNR is slower than the decline of W_{ini} , so the inner region of the SNR can be more turbulent than the region near the shock. As Geminga is now embedded in a strongly turbulent environment with $\delta B/B_0 > 1$, it should not be very closely behind the shock at present. This means the scale of the SNR should be larger than 90 pc now. We note that Geminga is in the southeast of Monogem Ring on the sky map (in the Galactic coordinate), and the distance of Monogem Ring is believed to be similar with that of Geminga. The ISM density in the south of Monogem Ring is derived to be 0.034 cm^{-3} (Knies et al. 2018), so we assume

that the SNR of Geminga has similar medium density n_{ISM} . Meanwhile, we assume $E_0 = 2 \times 10^{51} \text{ erg}$ for the progenitor of Geminga and get the current scale of the shock at $\sim 110 \text{ pc}$.

We solve Equation (9) numerically with the up-wind differencing scheme; Δt and Δr are set to be 1 kyr and 2 pc so that the scheme is stable even for a large $u_2(t)$. The calculated spatial distribution of $D(60 \text{ TeV})$ is shown in the right graph of Figure 3 in blue. As we are only interested in the downstream region of the shock, we simply set $D = D_{\text{ISM}}$ in the upstream region. The average $D(60 \text{ TeV})$ of the shaded area, namely the Geminga halo, is $3.8 \times 10^{27} \text{ cm}^2 \text{ s}^{-1}$ as measured by HAWC. We can see the diffusion coefficient just behind the shock is close to D_{ISM} , which indicates the current shock can no longer accelerate cosmic rays. This is consistent with the fact that the parent SNR of Geminga is not detected. Besides, since we have assumed $W_0 \sim v_s^2$, the downstream region near the shock should be much more turbulent in the early age of the SNR than the present day. At the age of 1000 yr of Geminga, our best $W_0(t)$ leads to $\delta B/B_0 \sim 7$ just behind the shock, if the outer scale of the turbulence is 5 pc. A large $\delta B/B_0$ should be common for young SNRs to ensure the effective acceleration of high energy particles. In the right of Figure 3, we also show the distribution of $D(60 \text{ TeV})$ in the case of a 90 pc current scale ($n_{\text{ISM}} = 0.034 \text{ cm}^{-3}$ and $E_0 = 0.8 \times 10^{51} \text{ erg}$) with a light blue line, assuming the same $W_0(t)$ with the former case. The average $D(60 \text{ TeV})$ for this case is larger than the result of HAWC.

We can also see from Figure 3, the distribution of $D(60 \text{ TeV})$ is very flat in the inner region of the SNR. This is because in the local rest frame, the downstream plasma has an outward velocity and has been following the shock wave. So the distribution of the diffusion coefficient should be ‘compressed’ towards the shock, compared with the case in which the downstream plasma is at rest in the local frame.

4 DISCUSSION

4.1 Other TeV halos

The mechanism to explain the slow diffusion around Geminga proposed in the previous section can be examined in other similar TeV γ -ray halos around pulsars. Besides Geminga there are other pulsars that are observed to be surrounded by slow diffusion halos in TeV. The spatial profile of γ -ray emission around PSR B0656+14 was reported by HAWC along with that of Geminga, and the indicated diffusion coefficient is 5 times larger compared with the Geminga case (Abeysekara et al. 2017a). While unlike Geminga, the associated SNR of PSR B0656+14, namely the Monogem Ring, is still observable in X-ray (Bunner et al. 1971; Plucinsky et al. 1996), as it is much younger than Geminga (~ 100 kyr). The position of PSR B0656+14 on the sky map is well inside the Monogem Ring, while the observation of the PWN of PSR B0656+14 suggests that the motion of the pulsar is almost parallel to the line of sight (Birzan et al. 2016). Since Monogem Ring is an extended structure with a scale of ~ 80 pc (Knies et al. 2018), the TeV halo of PSR B0656+14 can still be included by the SNR as long as its radial velocity is not faster than 600 km s^{-1} . If so, the origin of the slow-diffusion region may also be explained by the scenario of Section 3.

Vela X, as the PWN of Vela pulsar, is close to the center of Vela SNR (Sushch et al. 2011). H.E.S.S. has detected an extended TeV structure around Vela pulsar with a scale of ~ 6 pc (Aharonian et al. 2006; Abramowski et al. 2012), which is considered to be correlated with the X-ray filament (Hinton et al. 2011). The TeV halo is more extended than the X-ray filament, and the derived magnetic field is only $\sim 4 \mu\text{G}$, much smaller than that close to the pulsar (Hinton et al. 2011). So it is possible that the TeV structure is produced by the escaping electrons that are wandering in the turbulent environment inside the Vela SNR. Huang et al. (2018) also indicates that Vela X should be surrounded by a slow-diffusion environment, so that its lepton flux at the Earth will not conflict with the current experiments.

On the other hand, we pay attention to another source PSR B1957+20, around which no TeV structure has been detected so far. PSR B1957+20 is an old millisecond pulsar, which is definitely travelling in the ISM now. The bow-shock PWN associated to the pulsar has been detected by *Chandra* in 0.3–8 keV (Stappers et al. 2003; Huang et al. 2012), and the magnetic field of PWN is estimated to be $17.7 \mu\text{G}$ (Huang et al. 2012). So the parent electrons of the X-ray emission should be as high as tens of TeV, which means this PWN can indeed accelerate electrons to VHE. Besides, Aharonian et al. (1997) pointed out that ground based telescopes should be able to detect VHE γ -ray emission around the pulsar if the spin-down luminosity of the pulsar is larger than $10^{34} (r/1 \text{ kpc})^2 \text{ erg s}^{-1}$, where r is the distance of the pulsar. For the case of PSR B1957+20, r is inferred as 2.5 kpc (Cordes & Lazio 2002), and the spin-down luminosity of the pulsar is $7.48 \times 10^{34} \text{ erg s}^{-1}$ (Manchester et al. 2005), meeting the criterion above. All these imply that if the accelerated electrons are effectively confined near the source, TeV structure ought to be revealed. However, according to the present work, the VHE electrons may not be able to bound themselves by self-generation waves, and the turbulence in the ISM is far from adequate to confine the escap-

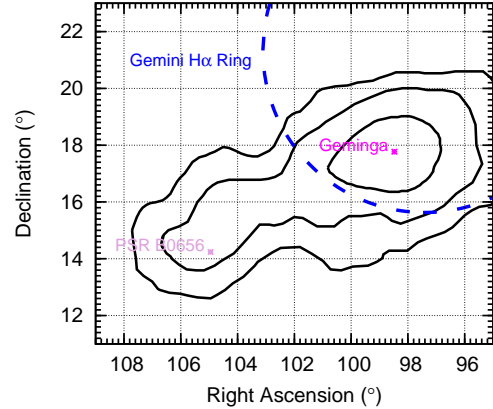


Figure 4. The positions of Geminga and the Gemini H α Ring on the sky map. The contours of the HAWC significance map between 1 and 50 TeV (5σ , 7σ , and 10σ) are shown in black (Abeysekara et al. 2017a). The blue dashed line represents the Gemini H α Ring (Knies et al. 2018).

ing electrons, unlike the case inside the SNR. Thus, plenty of electrons might have effectively spread out and the non-detection of VHE emission can be understood.

4.2 Is Geminga inside a stellar-wind bubble?

The scenario described in Section 3 may not be the unique possible case for a pre-existing slow-diffusion environment. It is also possible that Geminga is running into an unrelated turbulent region at present. Kim et al. (2007) discovered a large ring-like structure in H α emission that is centered at $(97.14^\circ, 21.33^\circ)$ in equatorial coordinates, dubbed the 'Gemini H α Ring'. As can be seen in Figure 4, the most intense part of the Geminga TeV halo is included by the Gemini H α Ring in projection. There is evidence that the Gemini H α Ring is interacting with the Monogem Ring (Kim et al. 2007). As the distance of Monogem Ring is estimated to be ~ 300 pc (Knies et al. 2018), the Gemini H α Ring should have a similar distance. Knies et al. (2018) pointed out that the Gemini H α Ring is most likely a stellar-wind bubble, as there are several OB type stars in the direction of the H α ring with distances of 200–350 pc. Meanwhile, the uncertainty of the trigonometric parallax of Geminga is still large, and the derived distance ranges from 190 pc to 370 pc (Faherty et al. 2007). Thus, Geminga is possibly inside the stellar-wind bubble now, and the shocked wind may provide Geminga a turbulent circumstance. Besides, the high ionization and low density environment of Geminga are also consistent with the features of stellar-wind bubble (Castor et al. 1975).

5 CONCLUSION

We study the possible origin of the slow-diffusion region around Geminga observed by HAWC. Considering the proper motion of Geminga, we verify that the mechanism of self-generated Alfvén waves due to streaming instability cannot work to produce such a low diffusion coefficient even

in the most optimistic scenario where the energy loss of electrons and the dissipation of the Alfvén waves are neglected. The reason is simple as Geminga is too weak to generate enough high energy electrons at the late age. We get an analytical result of the lower limit of the diffusion coefficient at 60 TeV, which are at most suppressed to about 0.2 times of the ISM value. This is much larger than the value required by the HAWC observation, which derives a diffusion coefficient hundreds times smaller than that of the ISM.

We further propose a scenario that the slow diffusion is an environment effect and Geminga is still inside its parent SNR, which is not identified at present. We show that if the ambient density is low, the scale of the SNR can be large enough to include Geminga and the TeV halo inside. We assume the magnetic turbulence is generated just behind the shock of the SNR with the Kolmogorov form, and the energy density of the turbulence is proportional to the square of the shock velocity. We solve the transport equation of the plasma wave downstream of the shock, and obtain the distribution of the diffusion coefficient inside the SNR. We find that Geminga can be reasonably embedded in a turbulent environment now, and the diffusion coefficient at 60 TeV can accommodate the result of HAWC. Another possible interpretation is also briefly presented, in which Geminga is now running into the stellar-wind bubble that creates the Gemini H α Ring.

We further discuss some other sources with TeV halos, such as PSR B0656+14 and Vela X. These cases also favor our new interpretation. It is still ambiguous if the inefficient diffusion region around pulsar is universal or not. As the ground-based Cherenkov instruments have identified plenty of VHE γ -ray sources associated with pulsars (of course many of them are PWNe rather than halos produced by escaping electrons) (Abeysekara et al. 2017b; H. E. S. S. Collaboration et al. 2018), we expect to investigate more cases in the future work. Besides, if energy-resolved observation of Geminga halo could be provided in the future, it is very helpful to give further judgement to the origin of the slow-diffusion region.

ACKNOWLEDGEMENT

We thank Prof. Hui Li for helpful discussion. This work is supported by the National Key Program for Research and Development (No. 2016YFA0400200) and by the National Natural Science Foundation of China under Grants No. U1738209, 11851303.

REFERENCES

Abdo, A. A., Allen, B., Berley, D., et al. 2007, *ApJ*, 664, L91
 Abeysekara, A. U., Albert, A., Alfaro, R., et al. 2017a, *Science*, 358, 911
 —. 2017b, *ApJ*, 843, 40
 Abramowski, A., Acero, F., Aharonian, F., et al. 2012, *A&A*, 548, A38
 Aguilar, M., Ali Cavasonza, L., Ambrosi, G., et al. 2016, *Physical Review Letters*, 117, 231102
 Aharonian, F., Akhperjanian, A. G., Bazer-Bachi, A. R., et al. 2006, *A&A*, 448, L43

Aharonian, F. A., Atoyan, A. M., & Kifune, T. 1997, *MNRAS*, 291, 162
 Bell, A. R. 1978, *MNRAS*, 182, 147
 Birzan, L., Pavlov, G. G., & Kargaltsev, O. 2016, *ApJ*, 817, 129
 Bunner, A. N., Coleman, P. L., Kraushaar, W. L., & McCammon, D. 1971, *ApJ*, 167, L3
 Caraveo, P. A., Bignami, G. F., De Luca, A., et al. 2003, *Science*, 301, 1345
 Castor, J., McCray, R., & Weaver, R. 1975, *ApJ*, 200, L107
 Cesarsky, C. J., & Kulsrud, R. M. 1981, in *IAU Symposium*, Vol. 94, *Origin of Cosmic Rays*, ed. G. Setti, G. Spada, & A. W. Wolfendale, 251
 Cordes, J. M., & Lazio, T. J. W. 2002, *ArXiv Astrophysics e-prints*, astro-ph/0207156
 D’Angelo, M., Blasi, P., & Amato, E. 2016, *Phys. Rev. D*, 94, 083003
 Drury, L. O. 1983, *Reports on Progress in Physics*, 46, 973
 Evoli, C., Linden, T., & Morlino, G. 2018, *ArXiv e-prints*, arXiv:1807.09263
 Faherty, J., Walter, F. M., & Anderson, J. 2007, *Ap&SS*, 308, 225
 Fang, K., Bi, X.-J., Yin, P.-F., & Yuan, Q. 2018, *ApJ*, 863, 30
 Gehrels, N., & Chen, W. 1993, *Nature*, 361, 706
 H. E. S. S. Collaboration, Abdalla, H., Abramowski, A., et al. 2018, *A&A*, 612, A1
 Han, J. L., & Qiao, G. J. 1994, *A&A*, 288, 759
 Hinton, J. A., Funk, S., Parsons, R. D., & Ohm, S. 2011, *ApJ*, 743, L7
 Hooper, D., Cholis, I., Linden, T., & Fang, K. 2017, *Phys. Rev. D*, 96, 103013
 Huang, R. H. H., Kong, A. K. H., Takata, J., et al. 2012, *ApJ*, 760, 92
 Huang, Z.-Q., Fang, K., Liu, R.-Y., & Wang, X.-Y. 2018, *ApJ*, 866, 143
 Kim, I.-J., Min, K.-W., Seon, K.-I., et al. 2007, *ApJ*, 665, L139
 Knies, J. R., Sasaki, M., & Plucinsky, P. P. 2018, *MNRAS*, 477, 4414
 Kulsrud, R. M., & Cesarsky, C. J. 1971, *Astrophys. Lett.*, 8, 189
 Leahy, D. A., & Williams, J. E. 2017, *AJ*, 153, 239
 López-Coto, R., & Giacinti, G. 2018, *MNRAS*, 479, 4526
 Malkov, M. A., Diamond, P. H., Sagdeev, R. Z., Aharonian, F. A., & Moskalenko, I. V. 2013, *ApJ*, 768, 73
 Manchester, R. N., Hobbs, G. B., Teoh, A., & Hobbs, M. 2005, *AJ*, 129, 1993
 Plucinsky, P. P., Snowden, S. L., Aschenbach, B., et al. 1996, *ApJ*, 463, 224
 Ptuskin, V. S., & Zirakashvili, V. N. 2003, *A&A*, 403, 1
 Ptuskin, V. S., Zirakashvili, V. N., & Plessner, A. A. 2008, *Advances in Space Research*, 42, 486
 Skilling, J. 1971, *ApJ*, 170, 265
 Stappers, B. W., Gaensler, B. M., Kaspi, V. M., van der Klis, M., & Lewin, W. H. G. 2003, *Science*, 299, astro-ph/0302588
 Sushch, I., et al. 2011, *A&A*, 525, A154
 Yuan, Q., Lin, S.-J., Fang, K., & Bi, X.-J. 2017, *Phys. Rev. D*, 95, 083007

APPENDIX A: NUMERICAL SOLUTION OF THE SELF-CONFINEMENT SCENARIO

Neglecting the proper motion of Geminga, we numerically solve the complete forms of Equation (1) and (2) in the following. The radiative cooling of electrons and the damping of Alfvén waves are considered, then Equation (1) and (2) are rewritten as

$$\frac{\partial N}{\partial t} - \nabla \cdot (D \nabla N) - \frac{\partial}{\partial E}(bN) = Q \quad (\text{A1})$$

and

$$\frac{\partial W}{\partial t} + v_A \nabla W = (\Gamma_{\text{cr}} - \Gamma_{\text{dis}})W. \quad (\text{A2})$$

The calculation of the cooling rate b is identical with that in Fang et al. (2018), and the Kolmogorov type wave dissipation rate is still adopted. In fact, for the ISM that is not influenced by the source, the wave growth and convection can be neglected, while the wave dissipation still exists. We universally add a compensatory growth term to keep intact the diffusion coefficient far from the source.

We solve Equation (A1) and (A2) iteratively in the one-dimensional scenario. For Equation (A1), we apply the operator splitting method to deal with the diffusion operator and the energy-loss operator separately. For each operator, we derive the differencing scheme with the finite volume method. This is important especially for the diffusion operator, as D can be changed abruptly in space. One may refer to Fang et al. (2018) for the details of the differencing schemes. The initial value of N is zero everywhere. For the boundary conditions, we set the the maximum injection energy to be 500 TeV. The typical scale of the Galactic random field is 100 pc, which means the one-dimensional diffusion is only valid within this scale around the source. If particles escape farther, the diffusion should switch to three-dimensional, and N will sharply declines. So we set the spacial outer boundary at 100 pc, namely $N(100 \text{ pc}) = 0$. The radius of the one-dimensional flux tube is assumed to be 1 pc. As to Equation (A2), we discretize it with the well-known upwind scheme. The initial W is decided by the diffusion coefficient in the ISM. To ensure the accuracy of the solutions, $D\Delta t/(\Delta x)^2$ and $v_A\Delta t/\Delta x$ should not be much larger than 1, where Δt is the time step and Δx is the radial step for both Equation (A1) and (A2). As $D_{\text{ISM}}(60 \text{ TeV}) \approx 3 \times 10^{30} \text{ cm}^2 \text{ s}^{-1}$, we set $\Delta t = 0.1 \text{ yr}$ and $\Delta x = 1 \text{ pc}$.

The spectral index γ of the injection spectrum and the mean magnetic field B_0 are important parameters for the self-confinement scenario. The former affects the growth rate of the Alfvén waves, while the later is decisive for the damping rate of the waves. In the left of Figure A1, we show the calculated $D(60 \text{ TeV})$ in the current age of Geminga with different γ and B_0 . For the case of harder γ (1.5) and smaller B_0 ($0.6 \mu\text{G}$), the diffusion coefficient around Geminga is significantly suppressed even in the current age, and the average D within 20 pc is comparative to the result of HAWC. As can be seen in the right of Figure A1, the diffusion coefficient declines quickly in the early age, then the wave damping dominates and the diffusion coefficient gradually rises.

However, in addition to the unrealistic assumption that Geminga is at rest, the assumption of one-dimensional diffusion is not always valid. The turbulence need to be weak, namely $\delta B \ll B_0$. The right of Figure A1 shows that in the early age of Geminga, the diffusion coefficient can be suppressed to very low value, corresponding to strong turbulence. When δB approaches B_0 , the diffusion mode should switch to three-dimensional, and the wave growth due to streaming instability is significantly reduced compared with the case of one-dimensional. This implies that the diffusion coefficient cannot be reduced to so low as calculated here, while a self-consistent calculation should be complex and beyond the scope of this work.

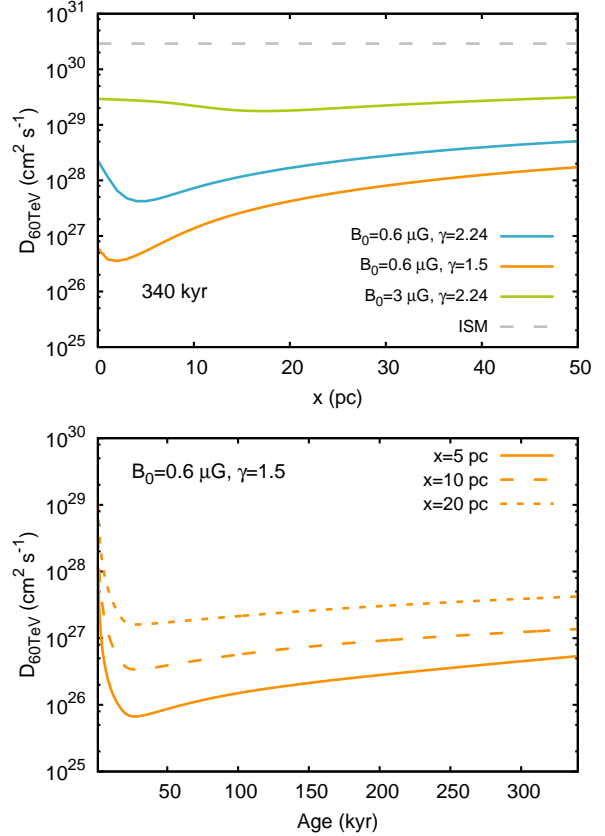


Figure A1. The result of the numerical solution to the self-confined propagation of electrons, assuming Geminga is at rest. Top: $D(60 \text{ TeV})$ in the current age of Geminga, for different combinations of B_0 and γ . Bottom: the evolution of $D(60 \text{ TeV})$ at different distances from Geminga.